Chapter 2

Integration of Remotely Sensed Images and Electromagnetic Models into a Bayesian Approach for Soil Moisture Content Retrieval: Methodology and Effect of Prior Information

Claudia Notarnicola and Romina Solorza

Additional information is available at the end of the chapter

http://dx.doi.org/10.5772/57562

1. Introduction

Remote sensing technologies in the microwave domain have shown the capability to detect and monitor changes related to Earth's surface variables, independently of weather conditions and sunlight.

Among these variables, soil moisture (SM) is one of the most requested ones [1]. This environmental variable is considered important to many ecological processes that occur on Earth's surface, from its relationship to climate events to its importance in terms of water availability for agricultural crops. In fact, it is considered an essential climate variable domain for the Global Earth Observation Climate (GCOS) [2]

At large scale, this biophysical variable is involved in weather and climate, influencing the rates of evaporation and transpiration. At medium-scale it influences hydrological processes such as runoff generation, erosion processes and mass movements and from the agriculture point of view determines the crops growth and irrigation needs. At small or micro-scale it has an impact on soil biogeochemical processes and water quality [3].

The ability to estimate soil moisture from satellites or airborne sensors is very attractive, especially in recent decades where the development of these technologies has taken a significant rise. This has led the possibility to have images with different spatial scales and repetition time. Despite numerous studies of moisture estimation have been developed using optical imaging, the most promising results have been obtained by using images from microwave sensors [1,4,5,6].

Satellite and aircraft remote sensing allow estimating soil moisture at large-scale, modeling the interactions between land and atmosphere, helping to model weather and climate with high accuracy [7]. In the last years many different approaches have been developed to retrieve surface soil moisture content from SAR sensors [1].

The estimation of soil moisture from SAR sensors is considered as an ill-posed problem, because many factors can contribute to the signal sensor response. The backscattering signal depends greatly on the moisture content, directly related to the dielectric constant of the soil (ε) and other factors such as soil texture, surface roughness and vegetation cover, being the latter the factors that may hinder a correct estimation of soil moisture [1].

Several studies have shown that soil moisture can be estimated from a variety of remote sensing techniques. However, only microwaves have the capability to quantitatively measure soil moisture under a variety of topography and vegetation [8]. The microwave remote sensing has demonstrated the ability to map and monitor relative changes in soil moisture over large areas, as well as the opportunity to measure, through inverse models, absolute values of soil moisture [1].

The sensitivity of SM in the microwave frequency is a well-known phenomenon, although it is still being studied by many research groups. Early researches conducted on the subject [9,10,11], among others, have shown that the sensors which operate at low frequencies of the electromagnetic spectrum, such as P or L band are capable of measuring soil moisture and overcome the influence of vegetation.

Currently most SAR systems on board of satellites (RADARSAT-2, COSMO-SkyMed, and TerraSAR-X) operate at C-and X-band, which are not the most suitable for the estimation of SM content. Some preliminary studies indicate the feasibility to estimate SM using this type of sensor, and specifically the new generation of X-band sensor [12]. However, working at such high frequencies involves dealing with interference effects introduced by the surface roughness, and especially vegetation coverage as part of the backscatter signal. Therefore, under these operating conditions, an estimate of the SM spatial variations is still a challenge.

Figure 1 shows the electromagnetic spectrum in the microwave region ordered according to the variable wavelength (in cm) and frequency (in GHz). In the same figure it is possible to have an overview of the major satellite missions, past, present and future, whose data have been used in numerous studies or can be used in the future to estimate SM.

The possibility of having multiple radar configurations was made possible thanks to the Envisat satellite launched by the European Space Agency (ESA) and its Advanced SAR (ASAR) sensor, operating in C-band [1]. Envisat/ASAR offered, unlike his predecessors, a great capacity in terms of coverage, incidence angles, polarizations and modes of operation, giving a great potential to improve the quality of many applications using SAR data.

Unfortunately, there are no current satellite missions in L band. ALOS, the satellite of Japan Aerospace Exploration Agency (JAXA), with PALSAR microwave sensor does not work since May 2011. At C-band, there is available data only from RADARSAT-2 of the Canadian Space Agency (CSA), because ERS-2 and Envisat from ESA stopped working in September 2011 and

http://dx.doi.org/10.5772/57562

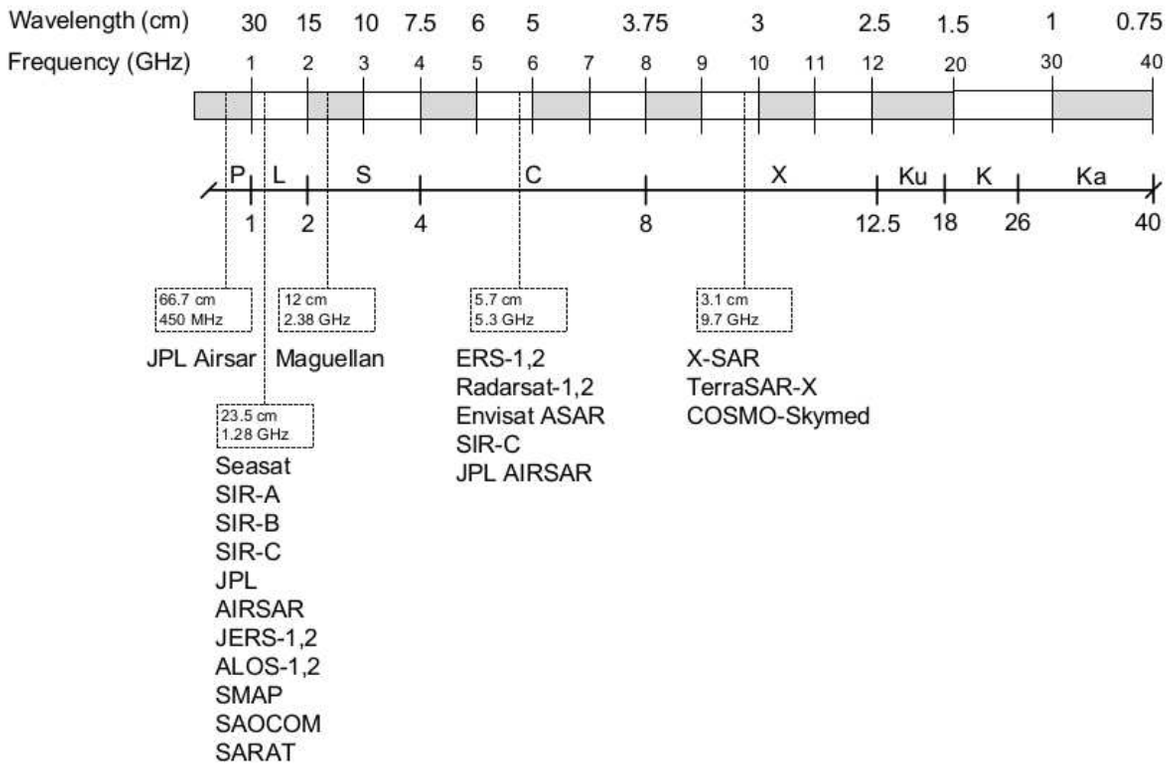

Figure 1. Main satellite missions (past, recent and future) designed in the microwave region of the electromagnetic spectrum (based on Richards, 2009).

April 2012, respectively. For the future nearby, there are expected data from planned L-band missions, such as Argentinian 1A and 1B SAOCOM, whose first launch is expected between 2014-2015; ALOS-2, which is expected to be launched in 2014. Also the SMAP active/passive satellite from the National Aeronautics and Space Administration (NASA), expected for end 2015, is very promising. SMAP will use high-resolution radar observations to disaggregate coarse resolution radiometer observations to produce SM products at 3 km resolution. The SM has been retrieved from radiometer data successfully using various sensors and platforms and these retrieval algorithms have an established heritage [7].

The most valuable information for the study of the SM has been obtained through the combination of different frequencies, polarizations and angles of incidence, as demonstrated in [11, 13,14,15]. The backscatter coefficient is highly sensitive to the micro roughness of the surface and vegetation coverage. These studies have been developed to determine the configuration of "optimal" sensor parameters, in terms of wavelength, frequency, polarization and angle of incidence to reduce interference of these factors when making an accurate estimate of SM.

In reference to specific studies, Holah et al. (2005) [16] found that an accurate estimate of SM can be achieved by using low or moderate (between 20° and 37°) incidence angles. Regarding polarizations, the most sensitive to SM are found to be HH and HV polarization while the less sensitive is VV. Li et al. (2004) [17] and Zhang et al. (2008) [18] found similar results. Furthermore Autret et al. (1989) [19] and Chen et al. (1995) [20] reported that the influence of surface roughness can be minimized by using co-polarized waves (HH/VV). Therefore, using multiple

polarizations should, in theory, improve the SM estimate. The general consensus of the literature indicates that low incidence angles, long wavelengths (such as L-band) and both HH and HV polarization settings are the most appropriate sensor for an accurate SM estimate [1].

Another effective approach to mitigate the ambiguity introduced by the vegetation and roughness is to focus attention on the temporal variations through time series of radar images. In this case the basis is to assume that the average roughness characteristics and vegetation remain almost unaltered while variations in moisture content affect backscatter signal along the time [21, 22]. In this regard, methods have been developed using change detection series, as in the recent study [23] Hornacek et al. (2012) used data from the wide swath Envisat/ASAR acquisition mode as part of an evaluation of the potential of algorithms for estimating SM for Sentinel-1 mission of ESA.

In remote sensing, researchers have to deal with two problems: the direct problem and the inverse problem. The direct problem refers to the development of electromagnetic models that can correctly characterize ground backscatter coefficient by using as input the sensor parameters, such as the angle of incidence (θ_i), the wavelength (λ) and a specified polarization configuration, as well as soil parameters, such as dielectric constant and roughness.

These models provide a solid physical description of the interactions between the electromagnetic waves and the objects on the Earth's surface (e.g., bare soil or vegetation), allowing to simulate numerous experimental settings in terms of sensor configurations and soil characteristics. The generality of models is a property essential to avoid dependence on local site conditions and characteristics of the sensor, a situation that often occurs when working with evidence-based algorithms.

Once the models have been validated, it is possible to develop algorithms to invert these models and predict soil surface properties using radar observations as inputs, which is the solution to the inverse problem [24,25,26].

Numerous backscattering models have been developed in recent decades to help determine the relationship between the measured signal at the sensor and biophysical parameters, with particular emphasis on understanding the effects of surface roughness [11, 25, 27]. Considering the inversion of the direct models many approaches have been developed through numerical simulations of forward models which include Look Up Tables, Neural Networks, Bayesian approaches, and minimization techniques.

For example, the potential of some of these approaches to provide accurate maps of SM has been investigated by Pampaloni et al. (2004) [28]. They conducted a performance comparison of the three inversion algorithms using time series of Envisat ASAR cross-and co-polarized images on a farm site in Italy. The algorithms evaluated for accuracy, error rate and computational complexity were: multilayer perceptron neural network, a statistical approach based on the Bayesian theorem and iterative optimization algorithm based on the Nelder-Mead method.

Among the different methods, the Bayesian approach has been deeply investigated for its capability to provide an evaluation of the uncertainties on the variable estimates as well as the possibility to create hierarchical models with different sources of information [11, 21, 29, 30].

http://dx.doi.org/10.5772/57562

The objective of this research is to examine the capability and accuracy of a Bayesian approach to retrieve surface SM setting different roughness and vegetation conditions in view of an operational use of the algorithm. Several implementations of the main algorithm were designed to evaluate their different capabilities to reproduce the ground reference data. In most cases, these approaches are based on the assumption of predefined behavior of some parameters, such as vegetation and roughness, measured in situ, and then used as conditional probabilities.

The developed method has been applied to two main test sites, one located in Argentina and the second in Iowa and exploited during the SMEX´02 campaigns. The comparison over two test sites is useful to have confirmation on the behavior of the developed algorithms.

The SMEX'02 test site was one of the first exploited to test the proposed methodology that was later extended to the Argentina test site.

For this reason larger space is given in this chapter to the Argentinean test site, where SM is being deeply studied because of the near future launch of the first SAOCOM satellite. In fact, there is a particular demand of SM maps from agricultural farmers of the Pampa region for monitoring the crop status, possible evaluation of water demand and yield assessment.

2. Remote sensing data and study areas

The proposed analysis is applied to two main datasets. The first dataset derives from an experiment carried out in Argentina in view of the SAOCOM mission. The second one is located in the USA and acquired during the SMEX'02 experiments where contemporary to SAR acquisitions intensively field campaigns were carried out.

2.1. Argentinean study area

The procedure adopted here was applied to data from SARAT L Band active sensor. The SARAT SAR is an airborne sensor (figure 2) used to simulate the SAOCOM images to be analyzed in feasibility studies. The SAR Airborne instrument works in L band (λ=23cm) and is fully polarimetric.

The data set consists of field soil moisture content measurements with the corresponding backscattering coefficients at HH, HV, VH and VV polarizations and 25° incidence angle acquired with a L-band SARAT sensor. SARAT project includes an airborne sensor and an experimental agricultural site. It is part of the SAOCOM mission of Argentinean Space Agency (CONAE). The main aim of the SARAT project is to provide full polarimetric SAR images to develop and validate different applications before the launch of the first satellite SAOCOM, the SAOCOM 1A, estimated for the year 2014. The SAR instrument is installed on a Beechcraft Super King Air B-200 from the Fueza Aérea Argentina (FAA) which has a nominal range of flight altitudes between 4000 and 6000 meters above the Earth's surface, resulting in the formation of images with angles of incidence between 20° and 70°.

Figure 2. SARAT instrument and Aircraft of the FAA.

This SAR system has the same characteristics of the upcoming SAOCOM. These characteristics are described on Table 1.

Central frequency	1.3 GHz (L band)
Chirp bandwidth	39.8 MHz
Pulse duration	10 μm
Pulse Repetition Frequency	250 Hz
Swath	9 km (nominal to 4200 m of height)
Azimuth resolution	1.2 m (nominal)
Slant Range resolution	5.5 m
Spatial resolution	6 m (nominal)
Polarization	Quad-Pol (HH, HV, VH y VV)
Incidence angle	20° - 70° (nominal to 4200 m of height)
Dynamic Range	45 dB
PSLR	-25 dB
Noise equivalent σ_0	-36.9 dB

Table 1. Technical characteristics of the SARAT sensor.

SARAT project also includes a validation sites in agricultural areas. For this study, an area inside the CETT (Teófilo Tabanera Space Center of CONAE) located in Cordoba province,

Argentina, was selected. Its central geographic coordinates are 31°31'15.08''S-64°27'16.32''W. Figure 3 shows the location of the test site.

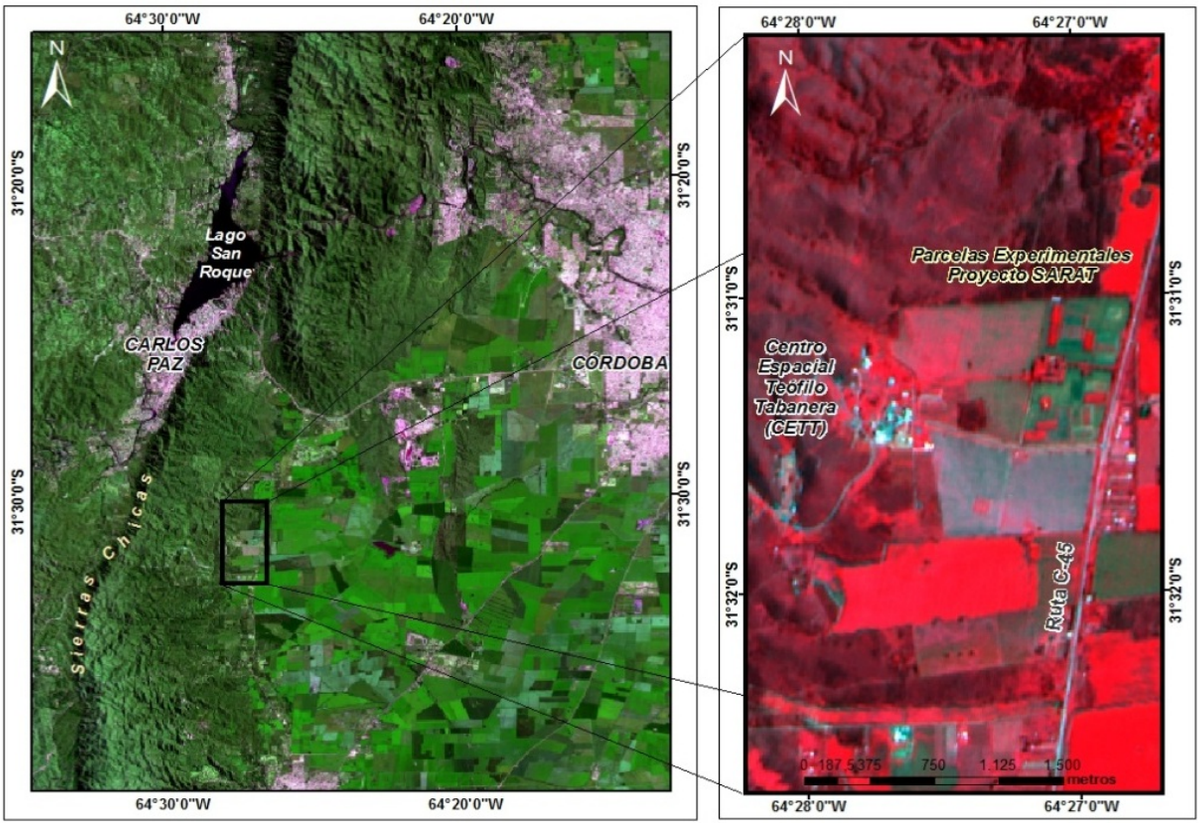

Figure 3. Location of the test site at Conae, in Argentina.

The experimental site, chosen for SM, vegetation and surface roughness measurements, has 10 fields with dimension of 50 m x 120 m which contain different kinds of crop and bare soil, as depicted in Fig. 4. All fields were intensively sampled during the SARAT acquisitions.

Plots with crops contain soybean, sunflower, corn and wheat crops. Figure 5 depicts crops stage at the moment of the SARAT acquisition time.

Some plots were left without vegetation to better investigate the interaction of microwave signal with roughness surfaces. The bare soil plots (1N, 2N, 1S and 2S) were ploughed with two roughness levels (low and high roughness) to evaluate the roughness impact on soil moisture retrieval at plot level, as shown in Fig. 6.

The roughness parameters, namely standard deviation of heights, s, and correlation length, l, were calculated as indicated in [31]. These parameters are listed in Table 2.

The SARAT images for this study (resolution: 9 m ground range) were acquired on February 2012 and all the data was provided by CONAE. Soil moisture varied between 4% and 40%, even though most plots showed medium-dry conditions.

Figure 4. Detail of the sampled plots during SARAT campaign acquisitions. N and S indicate North and South test fields.

Figure 5. Soybeans, wheat (winter development), corn and sunflower.

Figure 6. Bare plot with induced low (left) and high roughness (right).

Parameter	Symbol	High roughness value	Low roughness value
Rms height	s	3.22 cm	1.55 cm
Correlation length	l	8.17 cm	5.03 cm

Table 2. Mean roughness values inside the bare soil plots.

2.2. Iowa study area in the SMEX'02 experiment

SMEX'02 is a remote sensing experiment that was carried out in Iowa in 2002. The main site, chosen for soil moisture, vegetation and surface roughness measurements, was the Walnut Creek watershed, where 32 fields, 10 soybean and 21 corn fields, were sampled intensively [32]. The field and sensor data acquired during this experiment are particularly suitable thanks to the significant number of surveyed fields and wide range of soil conditions. The AirSAR images (resolution: 8-12 m ground range) were acquired on 1, 5, 7, 8, 9 July 2002. The five P-, L-and C-band images were processed by the AirSAR operational processor providing calibrated data sets.

3. Description of the methodology for SM estimation

The retrieval algorithm for SM is based on a Bayesian approach. Bayesian data analysis determines methods to make inference from data by using probabilities models for quantities.

The main characteristic of Bayesian methods is the explicit use of probability for quantifying uncertainty in inference based on statistical data analysis.

The process of Bayesian data analysis consists of three main steps:

- Definition of a joint probability model for all variables under evaluation;
- Calculate the posterior distribution which provides information on the unobserved quantities, given the observed data;
- Evaluation of the fit model.

Prior distributions can express our knowledge and uncertainty about the target variable. In this case the target variable could be thought as a random realization from the prior distribution.

The application of Bayesian approach implies passing from a prior distribution to a posterior distribution. Based on this concept, a relationship is expected between these two distributions [29, 30, 33]. A general feature of Bayesian inference is that the posterior distribution is centered at a point which represents a compromise between the prior information and the data. This compromise is strongly controlled by the data as the sample size increase.

A prior distribution may not have a population basis and for this reason it is desirable to have a prior which plays a minor role in the posterior distributions. These prior distribu-

tions are considered as flat, diffuse or non-informative. The rational to use such types of distributions is to let the inference being not affected by external information and based exclusively on data [34].

The proposed Bayesian approach is driven by both experimental data and theoretical electromagnetic models. The theoretical electromagnetic model has the main aim to simulate the sensor response by considering the characteristics of the soil and vegetation surface.

In order to have a better understanding of the proposed methodology, described in section 3.2, a brief description of the electromagnetic models is presented in the next section.

3.1. Electromagnetic modeling

The development of physical or theoretical models simulating direct backscatter coefficients in terms of soil attributes as dielectric constant and the surface roughness for an area of known characteristics is one of the most common approaches for SM estimation (Barrett et al., 2009). Electromagnetic models allow a direct relationship between the surface parameters and the backscattered radiation and are useful for understanding the sensitivity of the radar response to changes in these biophysical variables.

Despite its complexity, only theoretical models can produce a meaningful understanding of the interaction between electromagnetic waves and the Earth's surface. However, exact solutions of the equations that govern the rough surface scattering are not yet available and various approach methods have been developed with different ranges of validity [10]. The standard backscatter models are known as Kirchhoff Approximation (KA), which includes the Geometrical Optics Model (GOM), the Physical Optics Model (POM) and the Small Perturbation Model (SPM). These models can be applied to specific conditions of roughness in relation to the sensor wavelength. For example, GOM is considered for very rough surfaces, POM middle roughness surfaces and SPM smooth surfaces.

The Integral Equation Model (IEM), based on the radiative transfer model, has been developed by Fung and Chen in 1992 [27]. The model unifies the KA and the SPM model, a condition that makes it applicable to a wide range of roughness conditions. The IEM requires, as inputs, sensor parameters such as polarization, frequency and incidence angle, and target parameters such as the real part of the dielectric constant, the RMS height, s, and the correlation length, l [27].

For the IEM model, the like polarized backscattering coefficients for surfaces are expressed by this formula:

$$\sigma_{pp}^{0} = \frac{k^2}{2}\exp(-2k_z^2 s^2)\sum_{k=1}^{\infty}\left|I_{pp}^{n}\right|\frac{W^{(n)}(-2k_x,0)}{n!}, \tag{1}$$

where k is the wave number, θ is the incidence angle, $k_z=k\cos\theta$, $k_x=k\,\mathrm{sen}\,\theta$ and pp refers to the horizontal (HH) or vertical (VV) polarization state and s is the standard deviation of terrain

http://dx.doi.org/10.5772/57562

heights. The term I_{pp}^{n} depends on these parameters, k, s and on R_H, R_V, the Fresnel reflection coefficients in horizontal and vertical polarizations. The Fresnel coefficients are strictly related to the incidence angle and the dielectric constant. The symbol $W(-2k_x,0)$ is the Fourier transform of the n^{th} power of the surface correlation coefficient. For this analysis, an exponential correlation function has been adopted that seems to better describe the properties of natural surfaces [27].

For vegetated soils, the simple approach, based on the so-called Water Cloud Model (WCM), developed by [35] has been considered in this analysis. In this radiative transfer model, the vegetation canopy as a uniform cloud whose spherical droplets are held in place structurally by dry matter. The WCM represents the power backscattered by the whole canopy σ^0 as the incoherent sum of the contribution of the vegetation σ^0_{veg} and the contribution of the underlying soil σ^0_{soil}, which is attenuated by the vegetation layer through the vegetation transmissivity parameters τ^2. For a given incidence angle the backscatter coefficient is represented by the following expression:

$$\sigma^0 = \sigma^0_{veg} + \tau^2 \sigma^0_{soil}. \tag{2}$$

If the terms related to vegetation and incidence angle are explicitly written in more detailed way, the backscattering coefficients become:

$$\sigma^0 = A \cdot VWC^E \cos\theta \cdot (1 - \exp(-2 \cdot B \cdot VWC / \cos\theta)) + \sigma^0_{soil} \cdot \exp(-2 \cdot B \cdot VWC / \cos\theta), \tag{3}$$

where VWC is the vegetation water content (kg/m^2), θ the incidence angle, σ^0_{soil} represents the backscattering coefficient of bare soil that in this case calculated by using the IEM model, τ^2 is the two-way vegetation transmissivity with $\tau^2 = exp(-2B\ VWC/\ cos\theta)$. The parameters A, B and E depend on the canopy type and require an initial calibration phase where they have to be found in dependence of the canopy type and with the use of ground data.

In this work the model simulation enters directly in the inversion procedure. For the Bayesian approach, the simulated data are generated in order to compare them to the measured data and to create the noise probability density function (PDF) as detailed in the section devoted to this approach. For this reason, it is needed to perform a preliminary validation of the proposed model as their simulation enters directly the inversion procedure.

Calibration constant values of the WCM, namely A, B and E were taken initially from literature to take into account the effect of vegetation on the SAR signal [36]. Subsequently through a Maximum Likelihood approach they were determined to fit the data used in this work from both test sites. The application of calibration equations considers two different kind of vegetation, with respect to the sensor response: very dense vegetation (as corn and sunflower) and less dense vegetation (soybean and grass). This step includes the NDVI calculation from some SPOT and LANDSAT optical images for the Argentinean and SMEX'02 test site respec-

tively acquired close in time to the SAR image. Then the NDVI values were transformed in VWC through empirical approach defined by Jackson et al, 2004 [37].

The free parameters are illustrated in table 3, where also the RMSE of the difference between measured and simulated backscattering coefficients are reported. Figure 7 depicts the comparison between simulated and measured backscattering coefficients.

Model	A	B	E	RMSE
Soya	0.00119	0.03	0.634	1.7 dB
Corn	0.2	0.003	2.2	2.6 dB

Table 3. Calibration parameters for simulation of L band backscattering coefficients with the Water Cloud Model with distinction between soybean and corn types.

3.2. Bayesian approach for SM estimation

The objective of this research is to examine the capability and accuracy of a Bayesian approach to retrieve surface soil moisture under different assumptions for prior information on roughness and vegetation conditions in view of an operational use of the algorithm.

In the Bayesian approach, the scope is to infer biophysical parameters (e.g. soil moisture), from a set of backscattering responses measured by the sensor. The proposed algorithm is based on experimental data and theoretical models. The problem of having a few amounts of experimental data to build a reliable PDF has been overcome by the use of the simulated data from theoretical models. The Integral Equation Model (IEM) [27] was selected because it has the advantage of being applicable to a wide range of roughness scales. The general condition of validity of the model is $ks < 3$, where k is the wave number ($\approx 0.2732\ cm^{-1}$ for 1.3 GHz).

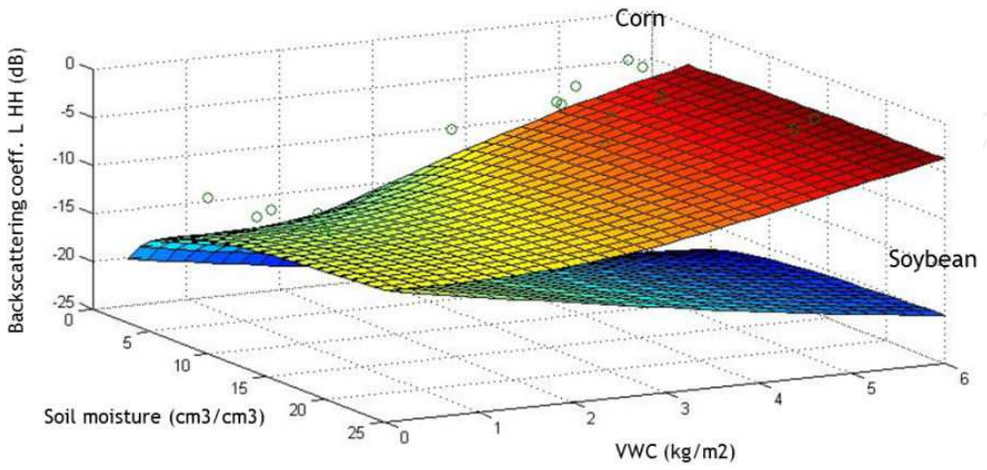

Figure 7. Comparison of measured backscattering coefficients (dots) with simulation from Water Cloud Model (surfaces) after the proper calibration of the free parameters. Two simulated surfaces are reported, one for corn (the red one) and the other soybean (the blue one).

http://dx.doi.org/10.5772/57562

For bare soil, these unknown parameters are the real part of the dielectric constant (ε), the standard deviation of the height (s) and the correlation length (l), the latter two describing the morphology of the surface. For vegetated fields, the Bayesian inversion was performed under two different approaches. In one case the Water Cloud Model (WCM) [35] is used to simulate the backscattering coefficients from vegetation. In the second case, the PDF parameters are properly modified to take into account vegetation effect through empirical relation with vegetation [38]. In both cases, the Vegetation Water Content (VWC) is added as unknown parameter, and it is derived from optical images. In this way, the approach exploits a synergy between SAR and optical images.

At the beginning, the conditional probability is assumed as normal distribution. In the training phase, the conditional PDF is evaluated using measured data (f_{im}) and simulated values from the IEM model (f_{ith}). The distribution assumption is then verified with a chi-squared statistics. The noise function N_I (eq. 4) and the related PDF parameters (mean and standard deviation) are calculated from the statistics of the ration between measured and simulated backscattering coefficients as follows [11, 39]:

$$N_i = \frac{f_{im}}{f_{ith}}. \tag{4}$$

Subsequently a joint PDF is obtained as a convolution of single independent PDFs. The joint PDF is a posterior probability derived from prior probability on roughness and soil moisture values and to the conditional probability which relates the variations of backscattering coefficients to variations of soil moisture and roughness. The relationship can be expressed as follows:

$$p\left(S_i \left| \sigma_i^0 \right.\right) = \frac{p_{prior}\left(S_i\right) p_{post}\left(\sigma_i^0 \left| S_i \right.\right)}{\int\limits_{S_i} p_{prior}\left(S_i\right) p_{post}\left(\sigma_i^0 \left| S_i \right.\right) dS_i}, \tag{5}$$

where the term at the denominator is a normalization factor with integration over all variables S_i. The variables Si can be:

- For bare soil: dielectric constant (ε), the standard deviation of the height (s) and the correlation length (l);
- For vegetated soil: dielectric constant (ε), the standard deviation of the height (s) and the correlation length (l), vegetation water content (VWC).

The variables σ^0_i refer to the input values derived from remote sensing data, which in the presented approach are:

- Backscattering coefficients at L-band HH and VV pol for the Argentinean test sites;

- Backscattering coefficients at C-band HH and VV pol, L-band HH and VV pol and the combination of C and L band at HH pol for SMEX'02 test site.

Based on the field data, the integration ranges for Bayesian inference were selected with different values as is illustrated in the following part. The main aim of using different intervals was to test the sensitivity of the methods to prior information, Through these integrations, to each pixel a value of dielectric constant is associated, starting from the corresponding backscattering coefficient values. Finally, with the formula proposed by [40] the dielectric constant values have been transformed to estimated values of soil moisture. The flowchart in Fig.8 outlines the main steps of the algorithm, including training and test phase.

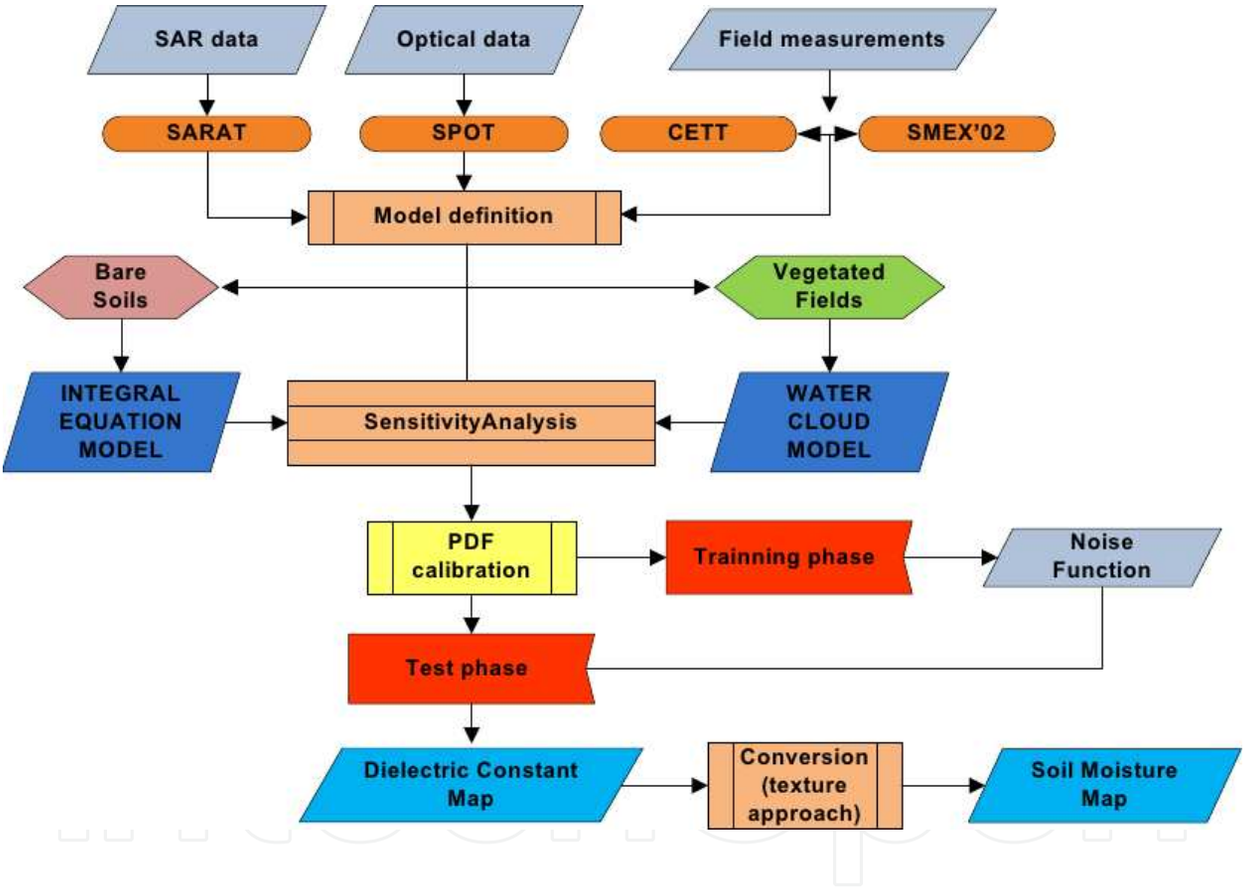

Figure 8. Flowchart of the Bayesian soil moisture approach applied to the Argentinean test site.

As above mentioned, another version of the Bayesian algorithm was developed to take into account the effect of vegetation into the PDF. The flowchart of the algorithm is the same as shown in fig.8, but instead of Water Cloud Model there is an adaptation of the PDF mean to an empirical function related to VWC as detailed described in Notarnicola et al., 2007 [38]. The algorithm was developed to work with C, L and combination of C and L band. In this work, this specific algorithm is applied to SMEX'02 data.

http://dx.doi.org/10.5772/57562

4. Results and discussion

The main aim of the work is to verify the sensitivity of the algorithm to prior conditions of roughness and vegetation in order to optimize the accuracy of the results. Based on this concept several retrievals were performed for different conditions of surface roughness, with specific algorithms for each coverage type in the study area. In the following the results on the Argentinean and SMEX'02 test sites are presented and discussed.

4.1. Argentinean test site

Over the Argentinean test site, the algorithm (fig.8) is divided in two main parts: one to be used in plots with bare soil or covered with sparse vegetation and another for vegetated soils. In both cases, two versions of the algorithm were developed: a simplified one working on a vector of mean values for each plot where the aim is to analyze the backscatter coefficient behavior using random values within ranges of s and l, and another one to work on the whole image, on pixel basis, to investigate the SM spatial distributions. Working with average values of backscattering coefficients has two objectives: to understand the effect on the SM estimates when the signal noise in the single plot is strongly reduced and to lower the computation burden when applying a random function for s and l variables.

An extensive analysis was conducted in order to understand the behavior of variables such as surface roughness and vegetation presence in the final SM estimation through the variability of the prior information. The different cases analyzed are listed below:

- Case 1: Pixel based algorithm for bare soil with fixed roughness. Three runs were executed: s=0.3 cm, l=5.0 cm; s=0.5 cm, l=5.0 cm and s=0.9 cm, l=5.0 cm. Then a mean value map is generated.
- Case 2: Pixel based algorithm for bare soil with an integration over a roughness range: 0.6 cm < s < 1.4 cm; l=5.0 cm.
- Case 3: Pixel based algorithm for bare soil with an integration over a roughness range: 0.6 cm < s < 1.4 cm; l=15.0 cm.
- Case 4: Pixel based algorithm for bare soil with an integration over a roughness range: 1.0 cm< s < 1.5 cm; l=5.0 cm. In this case a very small integration range was considered.
- Case 5: Algorithm applied to backscattering coefficients averaged at plot level with a random function. Values range: 0.5 cm < s < 1.2 cm; 5.0 cm < l < 10.0 cm.
- Case 6: VWC is calculated using a SPOT image. Fixed roughness and correlation length. s=0.5 cm; l=5.0 cm.
- Case 7: VWC is calculated using a SPOT image and a random function is implemented for s and l calculation, considering expected mean and standard deviation values for each parameter: mean value of s=0.7 cm and standard deviation value of 0.5 cm, mean value of l=5.0 cm and standard deviation of 5.0 cm. The random function is built as a noise function

added to the mean values of s and l. The pseudo random values are drawn from a standard normal distribution.

- Case 8: VWC is provided as an input variable and an integration is done over the following values: 0.01 <VWC < 6 Kg m^2.
- Case 9: VWC is calculated using a SPOT image, based on NDVI values, and an integration is done over roughness and correlation length in the following ranges:0.4 cm< s < 1.2 cm and 3.0 cm < l < 10.0 cm.

In Fig.9, preliminary results are presented where the different analyzed cases based on various prior conditions are numbered from 1 to 9. In general, for bare soil (fig. 9), the results showed a sensitivity of the algorithms to the different roughness conditions of each plot with a variability of around 5-7% (excluding the extreme cases). The highest variability among the cases is around 40% and is found when the roughness interval is very small (case 2 and 3). When considering a random function for roughness (case 7) and when performing the retrieval over average values of backscattering coefficients (case 5), the mean different with respect to ground measurements is around 15%.

For vegetated areas, due to the limited availability of field measurements (field 5N), the evaluation of the performances is still under work. More extensive results for vegetation are presented for the SMEX'02 experiments.

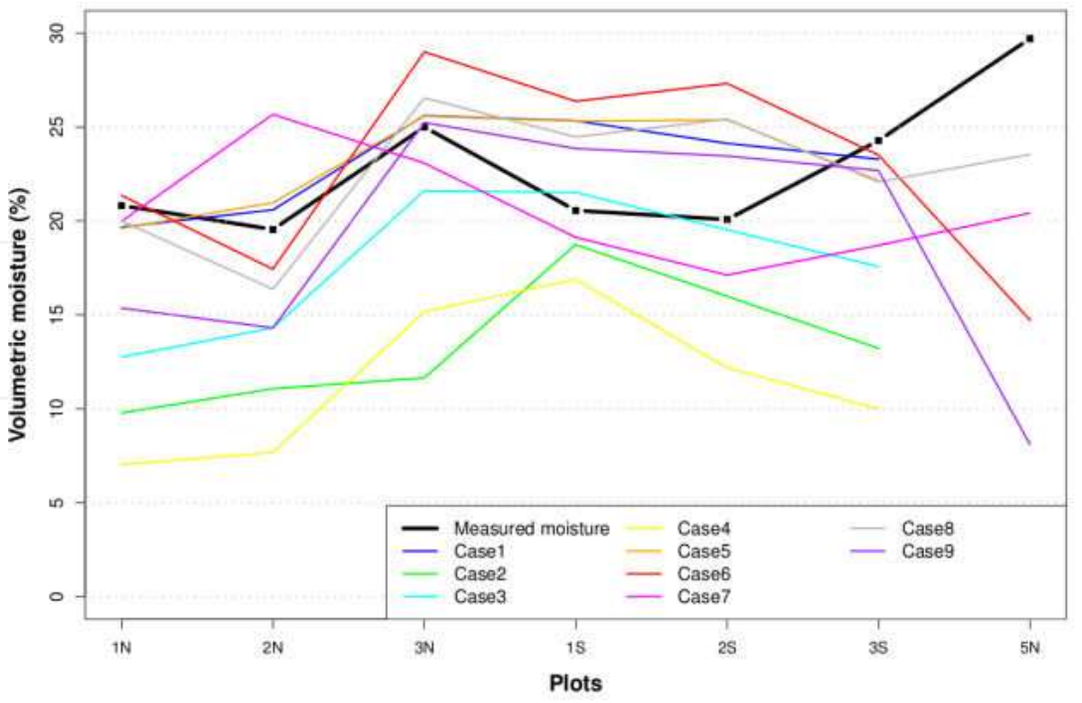

Figure 9. Comparison of SM estimates with measured values. Behavior diagram of the described cases.

http://dx.doi.org/10.5772/57562

Case1 and 3 results are reported in the form of SM maps in fig.10. A detailed analysis of the maps in fig.10 indicated error patterns detected for cases with rows of plots oriented orthogonally to the direction of the sensor observation. As it was observed, the backscattering coefficients for HH polarization is sensitive to the orientation of lines tillage and no inversion algorithms consider this factor. Consequently the results show significant errors in plots perpendicular to the observation.

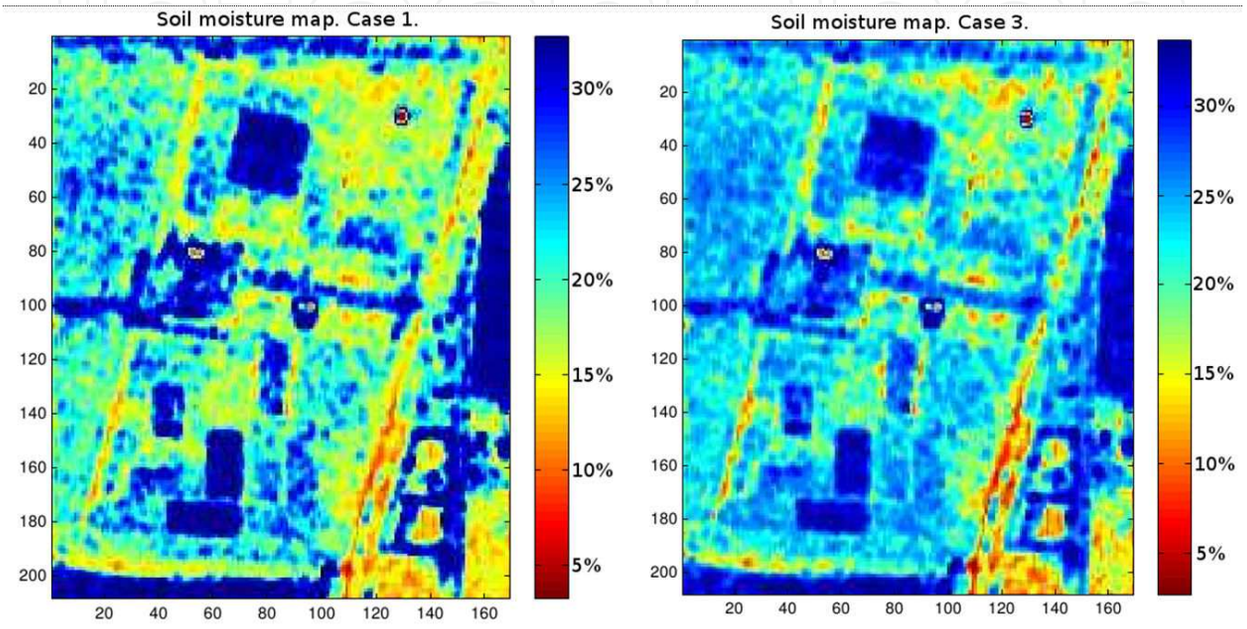

Figure 10. Soil moisture maps for Case 1 (left) and Case 3 (right) over the selected test site.

Case 1 shows that the northern plots with bare soils (1N and 2N) have moisture values very similar to the ground truth. On the contrary, southern plots with bare soils (1S and 2S) have higher moisture values than the measured ones, having the first of them a value of 25%, while the in situ data shown values around 20%. Case 3 shows that plot 1N and 2N obtained moisture values around 15%, which represents an over-estimation of the actual value of around 5%. For plots 1S and 2S, the estimate values are between 22 to 24%. Case 1 could model with good accuracy plots 1N and 2N losing accuracy in southern plots. On the contrary, Case 3 could model with relatively accuracy plots 1S and 2S losing precision in northern plots. The factor of apparent roughness change can be attributed to the orientation of the rows with respect to the SAR signal [41].

4.2. Results on the SMEX'02 experiments

As illustrated in previous paragraphs, the inversion methodologies based on Bayesian approach can be applied to different sensors configurations. In this way different polarizations and/or bands can be exploited to extract soil features. In fact, due to the different way C band or L band signals interact with soil and the above canopy layer, they are sensitive to different surface characteristics. Thus a proper combination of the two bands can help disentangle the

effect of vegetation and then improve the estimation of soil moisture. In this paragraph, the results of the Bayesian methodologies are illustrated and the evaluated in terms of:

- Correlation coefficients, R, between the estimates and the ground truth values
- Root Mean Square Error, RMSE, between the estimates and the ground truth values.

When dealing with the different cases due to the prior information, the retrieved values will be compared with the measurements through the Taylor plots [42].

The Bayesian approach has been applied to AirSAR data collected during the SMEX'02 experiments considering C band, L band and combination of C and L data.

The results for the estimation of SM are reported in table 4. As expected the estimation of SM is quite difficult, thus determining values of R varying from 0.47 to 0.80 for the combination of C and L bands. The highest difficulties are found for the detection and correct estimation of extreme values of soil moisture.

Configurations	Correlation coefficients	RMSE (cm^3/cm^3)
C band	0.47	0.10
L band	0.67	0.05
C + L band	0.80	0.02

Table 4. Correlation coefficients (R), RMSE for the comparison between the different estimates and ground truth values for SM values, excluding extreme values.

The retrieval of low values of SM can be difficult as the signal for soil is small and difficult to be disentangled from the vegetation signal. For high values, the signal from soil is strong but in the case of C bands the double bouncing and the effect of absorption from leaves also for L band, typical of narrow leaf plants such as soybean, determine a lower signal reaching the sensor [43]. The L band estimates are the only one able to predict highest values of SM.

Similar analyses were also found in Notarnicola et al. 2006 [39]. In this previous analysis, the methodologies were applied only to few fields of the same data set. With respect to the accuracy reported in Notarnicola et al., 2006 [39], a worsening in the performance is found. In particular the data set includes all the fields in the watershed basin and the fields located in the eastern part which exhibits anomalous values of SM, some very high values around 35% and some values lower than 5%. Considering the available meteorological information, the eastern and western parts of the watershed experienced very different intensity for the rain event where most of the rain event occurred in the western part.

If the watershed is divided in two parts the western and the eastern part the performances of the algorithm for SM retrieval differ significantly. The correlation coefficients are equal to 0.57 and 0.84, not significantly different from those found in [39].

Furthermore, the performances notably change if in the data set the soybean and corn fields are considered separately. The results are reported in table 5.

http://dx.doi.org/10.5772/57562

Configurations	Corn		Soybean	
	R	RMSE (cm^3/cm^3)	R	RMSE (cm^3/cm^3)
C band	0.36	0.127	*0.83*	*0.032*
L band	0.41	0.091	0.42	0.072
C+L band	*0.68*	*0.057*	*0.82*	*0.037*

Table 5. Correlation coefficients (R), RMSE for the comparison between the different estimates and ground truth values for SM values and for the Bayesian approach. With respect to table 4, in this case, the soybean and corn fields are considered separately. In italics, the values significantly different from the one found in whole data sets are indicated.

Similar characteristics are also found in [44], where it is proved that the RMSE is dependent on the level of vegetation of the different fields. Furthermore, in the case of C band, the signal coming from the VWC dominates over the signal coming from soil. In fact, when the vegetation has low value of VWC such as in the case of soybean fields, the C band is able to provide acceptable estimates for soil moisture. In the case of corn fields, the best results is obtained with the combination of C and L band, one sensitive to VWC and the other to the surface contribution. These discrepancies may be ascribed to the fact that in the Bayesian formulation the double bouncing between soil and corn trunk effect is not taken into account. This effect in such kind of plants with broad leaves could dominate [43].

On the SM estimates derived from combination of C and L band, a further analysis has been carried out by considering the effect of prior information on roughness.

More in details, the range of roughness in the integration of equation which is used to derive the expected values for soil moisture has been varied as follows:

- Low roughness: s varying between 0.2 and 1.2 cm;
- High roughness: s varying between 1.2 and 5.0 cm;
- Whole range of roughness: s varying between 0.2 and 5.0 cm.

The chosen values for roughness have selected based on prior information on roughness during field measurements. Along with these fixed ranges of roughness, a variable roughness interval has been considered based on the values of backscattering roughness. Higher values of backscattering coefficients on both C and L band have been also associated to high values of roughness.

The SM estimates derived from C and L band are illustrated in figure 11. When the estimates under these hypotheses are compared, they show an overall variability of around 25%. The results in term of correlation coefficients, are presented in the form of Taylor diagram as showed in fig. 12.

The SM estimates closest due to the ground measurements are those derived from the whole range of roughness and the adapted intervals. The high roughness and the whole range of roughness produces very close results both in terms of correlation coefficients and standard deviations.

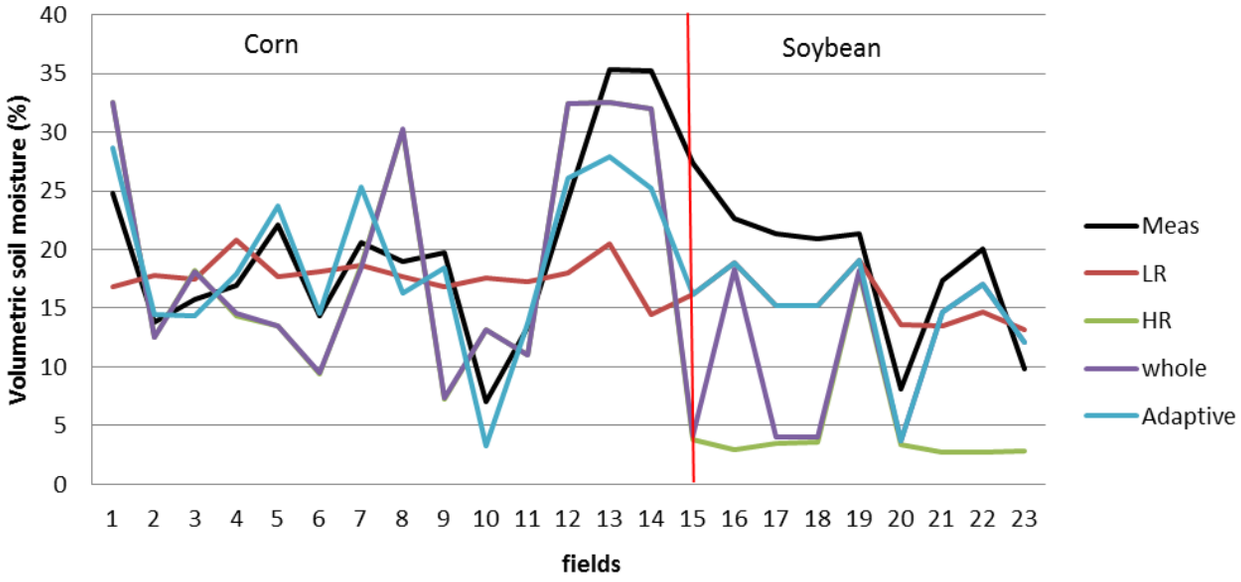

Figure 11. Comparison of SM estimates under different roughness hypothesis with ground measurements. "LR" stand for low roughness, "HR" for high roughness, "Whole" for the whole range of roughness and adaptive for adaptive values of roughness.

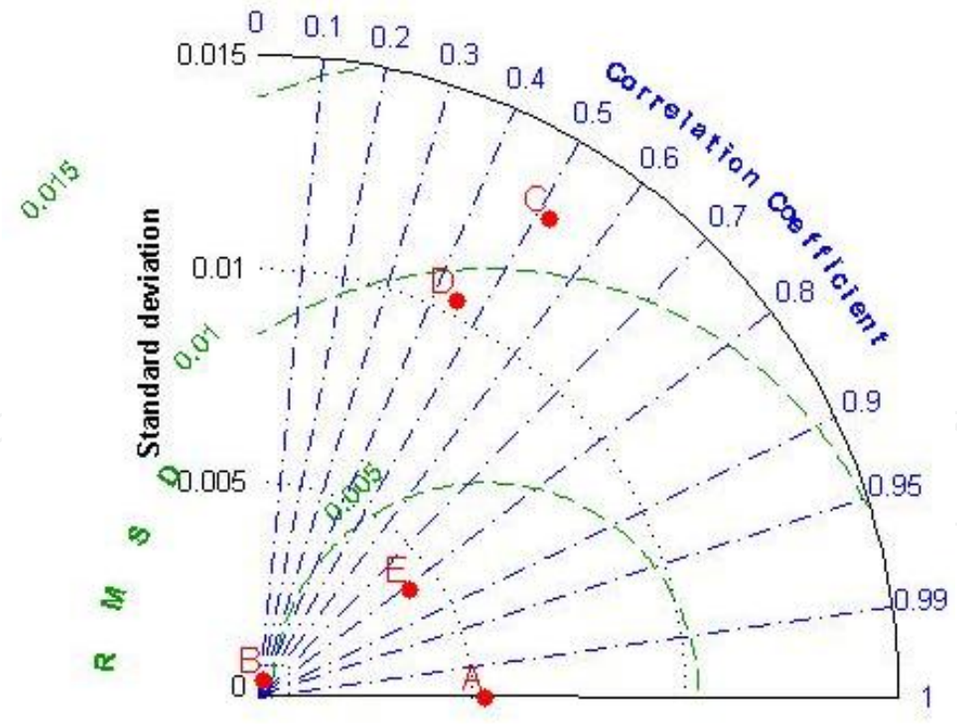

Figure 12. Taylor diagram showing the comparison under different prior hypotheses on roughness. A refers to ground measurements; B to low roughness; C to high roughness; D to whole range of roughness; E adapted roughness ranges.

http://dx.doi.org/10.5772/57562

5. Conclusions

The main objective of this chapter is to present the capability of Bayesian approach to estimate SM values starting from SAR backscattering coefficients. Two case studies are presented where SAR acquisitions took place over agricultural fields. The first case study was related to an Argentinean test site developed and equipped for acquisitions of airborne L band SAR called SARAT. The acquisitions were carried out in preparation of the SAOCOM mission. The second case study was related to the experiment SMEX'02 carried out in IOWA in 2002. In this experiment airborne AirSAR images were available and for this reason the retrieval was applied to C band, L band and C+L band data.

Based on the retrieval results, the main goal was then to verify the sensitivity of the SM estimates from the set prior information on roughness and vegetation. All the prior PDFs are set a uniform, non-informative but the set limits of the interval in the integration procedure can determine variation in the final SM estimates. This behavior is expected because the electromagnetic models used in the retrieval approach contain explicitly the dependence of backscattering coefficients on roughness and vegetation parameters.

The effect of prior information ranges from few percentages up to 25% where the highest sensitivity is found in both case studies when too specific and narrow intervals for roughness are used. The highest performances were found for both case studies when the range of roughness is large enough to include most roughness measurements. Moreover, if a preliminary assessment on the roughness level is available, the algorithm determines the highest performances with respect to the ground reference data.

An interesting feature observed in the case of Argentinean test site is the reduction of errors on the SM estimates when the retrieval is performed on average values of backscattering coefficients from each field. This behavior can be due to the reduction of noise present in the SAR signal.

As main conclusion of this analysis and suggestions in using the proposed the Bayesian algorithms for SM estimation, the following considerations emerge:

- The set of prior information has to be selected carefully;
- Even in the case of non-information prior PDF, the range of variability of the prior variable has an impact on the final estimates;
- It is preferable to integrate over a large interval of roughness and/or vegetation variables in order to take into account and properly weight all the measured values.
- As the speckle noise can influence the SM estimates, a proper filter over the SAR image needs to be applied before proceeding to the retrieval approach.

Acknowledgements

The authors wish to thank to CONAE and SAOCOM mission team for SARAT data provision and field measurements acquired during the remote sensing campaign.

Author details

Claudia Notarnicola[1*] and Romina Solorza[2]

*Address all correspondence to: claudia.notarnicola@eurac.edu

1 EURAC Research-Institute for Applied Remote Sensing, Viale Druso, Bolzano, Italy

2 Gulich Institute, CONAE, Falda del Carmen, Córdoba, Argentina

References

[1] Barrett B.W., Dwyer E., Whelan P. Soil Moisture Retrieval from Active Spaceborne Microwave Observations: An Evaluation of Current Techniques. Remote Sens., 2009; 1 210-242, doi:10.3390/rs1030210.

[2] World Meteorological Observatory, Climate Essential Variable http://www.wmo.int/pages/prog/gcos/index.php?name=EssentialClimateVariables (access 5 November 2013).

[3] Álvarez Mozos J., Casalí J., González A., López J. Estimación de la Humedad Superficial del Suelo mediante Teledetección de Radar en Presencia de una Cubierta de Cereal. Estudios de la Zona No Saturada del Suelo, 2005; VII 313–318.

[4] Engman E.T. Applications of microwave remote sensing of soil moisture for water resources and agriculture. Remote Sensing of Environment, 1991; 35 213–226,.

[5] Ulaby F.T., Aslam A., Dobson M.C. Effects of vegetation cover on the radar sensivity to soil moisture. IEEE Transactions on Geoscience and Remote Sensing, 1982; 20(4) 476–481.

[6] Lakshmi V. Remote Sensing of Soil Moisture. Hindawi Publishing Corporation ISRN Soil Science Volume 2013, Article ID 424178, 33 pages.

[7] Gruhier C., de Rosnay P., Hasenauer S., Holmes T., de Jeu R., Kerr Y., Mougin E., Njoku E., Timouk F., Wagner W., Zribi M. Soil moisture active and passive microwave products: intercomparison and evaluation over a Sahelian site, Hydrol. Earth Syst. Sci., 2010; 14 141–156.

[8] Behari J. Microwave Dielectric Behavior of Wet Soils. Anamaya Publishers, 2005.

[9] Ulaby F. T. Radar measurement of soil moisture content. IEEE Transactions on Antennas and Propagation, 1974; 22(2) 257–265. doi: 10.1109/TAP.1974.1140761.

[10] Ulaby F.T., Moore R.K., Fung A.K. Microwaves Remote Sensing: Active and Passive., volume III, Surface Scattering and Emission Theory. Artech House, Dedham, MA, 1986.

[11] Dubois P., Van Zyl J., Engman T. Measuring soil moisture with imaging radars. IEEE Transactions on Geoscience and Remote Sensing, 1995; 33 (4) 915–926.

[12] Baghdadi N., Aubert M., Zribi M. Use of TerraSAR-X Data to Retrieve Soil Moisture Over Bare Soil Agricultural Fields. IEEE Geoscience and Remote Sensing Letters, 2012; 9(3) 512–516.

[13] Dobson F.T. Ulaby L.E. Pierce, T.L. Sharik K.M. Bergen J. Kellindorfer J.R. Kendra E. Li Y.C. Lin A. Sarabandi K., Siqueira P.. Estimation of forest byophysical characteristics in northern michigancwith sir-c/x-sar. IEEE Transactions on Geoscience and Remote Sensing, 1995; 33 877–895.

[14] Ferrazzoli P., Paloscia S., Pampaloni P., Schiavon G. The potential of multifrequency polarimetric sar in assesing agricultural and arboreous biomass. IEEE Transactions on Geoscience and Remote Sensing, 1997; 35 5–17.

[15] Baronti S., Del Frate F., Ferrazzoli P., Paloscia S., Pampaloni P., Schiavon G.. SAR polarimetric features of agricultural areas. International Journal of Remote Sensing, 1995; 16 2639–2356.

[16] Holah N., Baghdadi N., Zribi M., Bruand A., King C.. Potential of ASAR/Envisat for the characterization of soil surface parameters over bare agricultural fields. Remote Sensing of Environment, 2005; 96 78–86.

[17] Li Z., Ren X., Li X., Wang L. Soil moisture measurement and retrieval using Envisat ASAR imagery. Proceedings of the IEEE International Geoscience and Remote Sensing Symposium (IGARSS 2004), 3539–3542, Anchorage, USA, 2004.

[18] Zhang T., Zeng Q., Li Y., Xiang Y. Study on relation between InSAR coherence and soil moisture. Proceedings of the ISPRS Congress, Beijing, China, 2008.

[19] Autret, Bernard R., VidalMadjar D.. Theoretical study of the sensitivity of the microwave backscattering coefficient to the soil surface parameters. International Journal of Remote Sensing, 1989; 10 171–179.

[20] Chen K.S., Yen S.K., Huang W.P.. A simple model for retrieving bare soil moisture from radar scattering coefficients. Remote Sensing of Environment, 1995; 54 121–126.

[21] Pierdicca N., Pulvirenti L., Bignami C.. Soil moisture estimation over vegetated terrains using multitemporal remote sensing data. Remote Sensing of Environment, 2010; 114 440–448.

[22] Balenzano A, Satalino G., Belmonte A., D'Urso G., Capodici F., Iacobellis V., Gioia A., Rinaldi M., Ruggieri S., Mattia F. On the use of multitemporal series of COSMO-SkyMed data for LANDcover classification and surface parameter retrieval over agricultural sites. Proceeding of Geoscience and Remote Sensing Symposium (IGARSS), 142–145, July 2011.

[23] Hornacek M, Wagner W, Sabel D, Truong H.L, Snoeij P, Hahmann T, Diedrich E, Doubkova M. Potential for High Resolution Systematic Global Surface Soil Moisture Retrieval Via Change Detection Using Sentinel-1. IEEE Journal of Selected Topics in Applied Earth Observations and Remote Sensing, 2012, 1–9.

[24] Dobson M.C., Ulaby F. T.. Mapping Soil Moisture Distribution With Imaging Radar, chapter 8, 407–433. John Wiley and Sons Inc., 1998.

[25] Shi J., Wang J., Hsu A.Y., ONeill P.E., Engman E.T.. Estimation of bare surface soil moisture and surface roughness parameter using l-band SAR image data. IEEE Transactions on Geoscience and Remote Sensing, 1997; 35 1254–1266.

[26] Oh Y.. Quantitative retrieval of soil moisture content and surface roughness from multipolarized radar observations of bare soils surfaces. IEEE Transactions on Geoscience and Remote Sensing, 2004; 42(3) 596–601.

[27] Fung, A. K. Microwave Scattering and Emission Models and their Application. Artech House, Boston; 1994.

[28] Pampaloni P., Santi E., Paloscia S., Pettinato S., Poggi P. Radar Remote Sensing of Soil Moisture, ENVISNOW Project, SMC algorithms. Technical report, IFAC-CNR, October 2004.

[29] Notarnicola C., Posa F. Bayesian algorithm for the estimation of the dielectric constant from active and passive remotely sensed data. IEEE Geoscience and Remote Sensing Letters, 2004; 1(3) 179–183.

[30] Paloscia S., Pampaloni P., Pettinato S., Santi E. A comparison of algorithms for retrieving soil moisture from ENVISAT/ASAR images. IEEE Transactions on Geoscience and Remote Sensing. 2008; 46(10) 3274-3284.

[31] Barber M., Grings F., Perna P., Bruscantini C., Karszenbaum H. Análisis de las mediciones de rugosidad del Centro Espacial Teófilo Tabanera, Córdoba. Technical report, CONAE-IAFE,Mayo

[32] http://nsidc.org/data/amsr_validation/soil_moisture/smex02/

[33] Barber M., Grings F., Perna P., Piscitelli M., Maas M., Bruscantini C., Jacobo-Berlles J., Karszenbaum H. Speckle Noise and Soil Heterogeneities as Error Sources in a Bayesian Soil Moisture Retrieval Scheme for SAR Data. IEEE Journal Of Selected Topics In Applied Earth Observations And Remote Sensing, 2012; 5(3).

[34] Gelman A., Carlin J.B., Stern H.S., Rubin D. B., Bayesian data analysis, Chapman&Hall/CRC 1995.

[35] Attema E. P, Ulaby F.T.. Vegetation Modeled as a Water Cloud. Radio Science, 1978; 13(2) 357–364.

[36] Dabrowska-Zielinska K., Inoue Y., Kowalik W., Gruszczynska M.. Inferring the effect of plant and soil variables on C-and L-band SAR backscatter over agricultural fields, based on model analysis. Advances in Space Research, 2007; 39 139–148.

[37] Jackson T., Chen D., Cosh M., Li F., Anderson M., Walthall C., Doriaswamy P., Ray Hunt E. Vegetation water content mapping using Landsat data derived normalized difference water index for corn and soybeans. Remote Sensing of Environment, 2004; 92 475–482.

[38] Notarnicola, C. & Posa, F. Inferring vegetation water content from C and L band images, IEEE Transactions on Geoscience and Remote Sensing, 2007; 45(10) 3165-3171.

[39] Notarnicola C., Angiulli M., Posa F. Use of Radar and Optical Remotely Sensed Data for Soil Moisture Retrieval on Vegetated Areas. IEEE Transactions on Geoscience and Remote Sensing, 2006; 44(4) 925-935.

[40] Hallikainen M.T., Ulaby F.T., Dobson M.C., El Rayes M.A., Wu L.K.. Microwave dielectric behavior of wet soil-part 1: Empirical models and experimental observations. IEEE Transactions On Geoscience And Remote Sensing, 1985; GE-23(1) 25–34.

[41] Solorza R., Notarnicola C., Karszenbaum H., Retrieval of soil moisture using a Bayesian approach and electromagnetic models in views of the SAOCOM mission: study on SARAT images in an agricultural site in Argentina, Proceeding of Igarss 2013, July 2013, Melbourne, Australia.

[42] Taylor, E, K, Summarizing multiple aspects of model performance in a single diagram, Journal of Geophysical Research, 2001; 106(D7), 7183-7192.

[43] Macelloni G., Paloscia S., Pampaloni P., Marliani F., Gai, M. The relationship between the backscattering coefficient and the biomass of narrow and broad leaf crops, IEEE Transaction on Geoscience and Remote Sensing, 2001; 39(4) 873-884.

[44] Lakhankar T., Ghedira H., Temimi M., Sengupta M., Khanbilvar R., Blake, R. Non-parametric methods for soil moisture retrieval from satellite remote sensing data, Remote Sensing, 2009; 1, 3-21. doi: 10.3390/rs1010003.

IntechOpen